Simultaneous improvements of the strength and ductility of fine-grained AA6063 alloy with increasing number of ECAP passes

Samaee, M.; Najafi, S.; Eivani, A. R.; Jafarian, H. R.; Zhou, Jie

DOI
10.1016/j.msea.2016.05.070

Publication date
2016

Document Version
Accepted author manuscript

Published in
Materials Science and Engineering A: Structural Materials: Properties, Microstructures and Processing

Citation (APA)
Samaee, M., Najafi, S., Eivani, A. R., Jafarian, H. R., & Zhou, J. (2016). Simultaneous improvements of the strength and ductility of fine-grained AA6063 alloy with increasing number of ECAP passes. Materials Science and Engineering A: Structural Materials: Properties, Microstructures and Processing, 669, 350-357. https://doi.org/10.1016/j.msea.2016.05.070

Simultaneous improvements of the strength and ductility of fine-grained AA6063 alloy with increasing number of ECAP passes

M. Samaee[1], S. Najafi[1], A.R. Eivani[1], H.R. Jafarian[1 *], J. Zhou[2]

[1] School of Metallurgy and Materials Engineering, Iran University of Science and Technology (IUST), Tehran, Iran

[2] Department of Biomechanical Engineering, Delft University of Technology, Mekelweg 2, 2628 CD Delft, The Netherlands

Abstract

In this research, grain refinement through severe plastic deformation (SPD) in combination with a thermal treatment to create a fine initial grain structure with a high degree of supersaturation was taken as a viable approach to achieving simultaneous increases in the hardness, strength and ductility of the aluminum alloy AA6063 during further SPD. A recrystallized structure with grain sizes around 20 µm was obtained after two passes of equal channel angular pressing (ECAP), followed by a thermal treatment at 500 °C for 10 s and water quenching. The alloy with the supersaturated α-Al matrix was subjected to further ECAP processing up to six passes to create a cellular structure on a nano scale. Hardness and tensile tests revealed the changes of hardness, strength and ductility along with increasing number of ECAP passes. It was found that after two ECAP passes, the ductility of the alloy decreased from the value after the prior two-pass ECAP and thermal treatment. However, by further ECAP processing up to six passes, the ductility increased along with the increases in hardness and strength. The remarkable improvement in ductility

* Corresponding author. Email: jafarian@iust.ac.ir; Tel: +98 21 77 240 540; Fax: +98 21 77 240 480.

was attributed to a nanosized cellular structure with a large area of high-angle grain boundaries developed from the fine initial grain structure formed during the two-pass ECAP and thermal treatment applied earlier.

Keywords

Aluminum alloy; Severe plastic deformation (SPD); Equal channel angular pressing (ECAP); Thermal treatment; Nanocrystalline structure; Strength; Ductility.

1 Introduction

Significant improvements in the strengths of a wide range of metallic materials have been achieved through severe plastic deformation (SPD) [1–7]. Regardless of the level of the strength of a metallic material, for engineering applications, a reasonable ductility is always needed to ensure an acceptable fracture toughness and to prevent catastrophic failure from taking place. Despite the critical importance of ductility, the vast majority of the studies on SPD for various engineering materials are primarily concerned with the improvement in strength [1–7]. Poor ductility is often regarded as an inherent property of ultra-fine grained (UFG) or bulk nanostructured (BN) metals and alloys processed by means of SPD. When these materials are considered for real engineering applications [1–7], however, the loss in ductility accompanies by the gain in strength through SPD is a serious concern. Only a few researchers have reported the improvements in ductility after SPD and the most important data are gathered in two review papers [8,9].

To achieve simultaneous improvements in strength and ductility, a number of approaches may be taken. Panigrahi and Jayaganthan [10], for example, combined short annealing and

aging treatments with cryorolling to improve the strength and ductility of an Al-Mg-Si alloy. Zha et al., [11,12] made use of interpass annealing during the interval of equal channel angular pressing (ECAP) to enhance the ductility of an Al-Mg alloy. Wang et. al., [13] achieved improved tensile elongation by creating a bimodal grain size distribution of nanostructured copper after a thermomechanical treatment. In most cases [10][11,12] [13], an improvement in ductility was made at the expense of strength improvement achievable through SPD. Nevertheless, the feasibility of achieving an optimum trade-off between strength and ductility has encouraged the further developments of UFG and BN materials as well as various SPD processes, and opened up a lot of potential for these advanced materials to be used as high-performance structural materials.

The present research was aimed at simultaneous improvements in ductility and strength for an aluminum alloy processed by ECAP. The key to realizing the improvements lay in creating a fine initial grain structure with a high degree of supersaturation. It was based on the earlier finding [14] that the tensile elongation of the AA6063 alloy could be enhanced, if a fine grained structure was produced with the alloying elements (mainly Mg and Si) in the α-Al solid solution and the gained elongation would decrease with increasing extent of the precipitation of second-phase particles. In the light of this finding, in the present research, a fine initial grain structure with large amounts of the alloy elements in the α-Al solid solution was produced by applying ECAP and a thermal treatment to allow recrystallization to take place and prevent second-phase particles from precipitating. Then, the developments of nanostructure, hardness and tensile properties, i.e., yield (YS) and ultimate tensile strength (UTS) and elongation, along with further ECAP passes, were investigated.

2 Experimental Procedure

The AA6063 aluminum alloy was received in the form of an extruded rod with a diameter of 100 mm. Its chemical composition in comparison with the nominal composition is given in Table 1. The rod was cut into 140 mm long pieces. The latter were machined into cylindrically shaped billets with a diameter of 20 mm, solution-treated at 550 °C for 30 min and quenched in water in order to eliminate the effects of prior thermal and mechanical processing history on the microstructure and mechanical behavior of the alloy.

Table 1: Chemical composition of the AA6063 alloy used in this study.

Element (wt. %)	Al	Mg	Si	Fe	Cu	Mn	Cr	Zn	Ti
AA6063 used in this study	Balance	0.84	0.57	0.31	0.03	0.04	0.03	0.10	0.03
Nominal composition of AA6063	Balance	0.45-0.9	0.2-0.6	Max 0.35	Max 0.1	Max 0.1	Max 0.1	Max 0.1	Max 0.1

For ECAP, a split die with a cone-shaped outside was inserted into a die holder. The diameter of the channels of the ECAP die was 20 mm. The channel intersection angle was 90° and the outer corner curvature angle 22.5°. A strain of one was imposed on the billet at each ECAP pass [15]. ECAP was performed at room temperature and at a ram speed of 1 mm/s.

To produce a fine initial grain structure, the billets were subjected to two ECAP passes and then a thermal treatment at 500 °C for 10 s. With this thermal treatment, most of the alloying elements were brought into the α-Al solid solution and no significant grain growth

could occur [14]. The solution-treated billets were fed into the ECAP machine and deformed through six passes at room temperature.

The microstructures of the material at different processing steps were examined using a polarized light microscope. Samples were cut along the longitudinal axis of the billet and prepared, following a standard procedure of grinding and polishing. To reveal microstructural details, polished samples were etched using a HBF_4 solution at 20 V.

Brinell hardness was measured on a plane normal to the ECAP direction. 20 indentations were made for each sample and the average value was obtained. Sub-size flat specimens were prepared for tensile testing according to ASTM E8. However, due to the size limit, i.e., the short length of the specimen, especially after a large number of ECAP passes, all the dimensions were reduced by 50% in order to facilitate the extraction of tensile specimens from ECAP processed billets. The tensile specimens with a total length of 50 mm and a grip section length of 15 mm had a gauge length of 12.5 mm, a width of 3 mm and a thickness of 2 mm. A SANTAM universal testing machine was used for tensile testing at a crosshead speed of 0.7 mm/min. Load-displacement data were obtained and converted to engineering stress-strain curves. 0.2% yield strength (YS), ultimate tensile strength (UTS), uniform elongation (e_u) and elongation to failure (e_f) were determined [16]. True stress-strain data were calculated by correcting the stresses in the localized deformation region using a power curve relation:

$$\sigma = K\varepsilon^n \quad (1)$$

where σ and ε are the effective stress and strain, respectively. The values of strain hardening exponent *n* and strength coefficient *K* were estimated in the uniform deformation region of the curves, i.e., after yielding and before necking.

The cellular structures of the material after different passes of ECAP were revealed by means of electron backscatter diffraction (EBSD). Samples were prepared, following the conventional procedure, starting from mechanical grinding and ending up with electrolytic polishing (20 V; 10 sec; flow rate: 15; electrolyte: 700ml CH_3OH + 300 ml HNO_3; temperature: 243 K). EBSD analysis was performed using a JEOL 7100F scanning electron microscope (accelerating voltage: 15 kV; tilt angle: 70 °; working distance: 15 mm; step sizes: 0.05 µm). Orientation contrast data were analyzed with the TSL OIM analysis software. Subgrains were determined by setting a cut-off value of 15 ° as the minimum misorientation angle of high angle grain boundaries (HAGBs). The minimum misorientation angle of low angle grain boundaries (LAGBs) was set at 2 °.

3 Results and Discussion

3.1 Formation of a fine initial grain structure after the two-pass ECAP and thermal treatment

As described earlier, the as-received extruded rod was first solution-treated at 550 °C for 30 min to remove the effect of all previous thermal and mechanical processing history on the material. As a result of the high-temperature treatment, a fully recrystallized, coarse grain structure was formed, as shown in Fig. 1. The average grain size was measured to be 238 µm by using the intercept method.

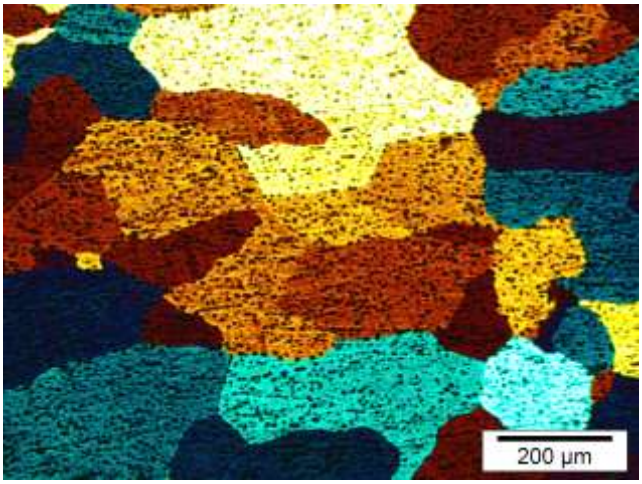

Figure 1 Grain structure of the as-received extruded rod after a thermal treatment at 550 °C for 30 min, followed by quenching in water.

To obtain a fine initial grain structure for further SPD, the material was ECAP-processed through two passes and then solution-treated again. Apparently, a lower thermal treatment temperature (but above the recrystallization temperature of the AA6063 alloy – 320 ^{0}C) would result in a finer recrystallized grain structure. However, such a treatment would require a longer time for recrystallization to complete, e.g., 10 min at 420 °C, which would cause the alloying elements in the α-Al matrix to lose partially and coarse second-phase particles to precipitate [14]. Consequently, the alloy would become softer as a result of reduced solution hardening and its precipitation hardenability to be exhibited during aging would be reduced as well. Based on the considerations on strength, a short thermal treatment at a high temperature would be preferred.

In a previous investigation on the annealing of the AA6063 alloy [14], it was found that the tensile elongation of AA6063 increased if a large fraction of the alloying elements were kept in the α-Al solid solution. This was attributed to a stronger work-hardening effect contributed by a higher concentration of the alloying elements in the α-Al solid solution, which postponed localized deformation and necking during tensile testing. In addition, the

elongation to failure increased, when a fine initial grain structure was created, because of a greater capacity of grain boundaries to accommodate dislocations formed during tensile deformation and to postpone fracture [14]. A fine grain structure is usually obtained when thermal exposure temperature is low, e.g., at 350 or 420 °C. For the material solution-treated at such a low temperature, however, elongation may decrease because of the formation of a large fraction of second phase particles and the partial depletion of the alloying elements in the α-Al matrix [14]. The consideration on elongation also suggested a short high-temperature thermal treatment in order to keep grains fine and prevent second phase particles from precipitating. On the other hand, the results obtained from the previous investigation on the annealing behavior of this alloy [14] indicated that abnormal grain growth tended to occur if the annealing temperature exceeded 500 °C and the material was annealed for 30 s. Therefore, a thermal treatment at 500 °C for 10 s, which is below the typical temperature of solution treatment for AA6xxx series alloys (520-580 °C), was chosen.

The fine initial grain structure after the two passes of ECAP, followed by the thermal treatment at 500 °C for 10 s is shown in Fig. 2. The average grain size of the material prior to further ECAP was 20 μm.

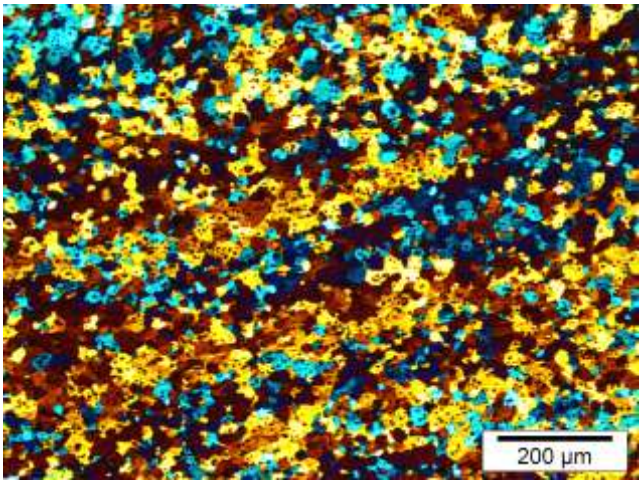

Figure 2 Grain structure of the material after the two-pass ECAP and thermal treatment at 500 °C for 10 s, followed by quenching in water.

3.2 Development of nanostructure during subsequent ECAP

EBSD maps showing the grain and cellular structures of the material after two and six passes of ECAP are presented in Fig. 3, in which the red color and black color are used to differentiate between low angle grain boundaries (LAGBs) between 2 and 15 ° and high angle grain boundaries (HAGBs) above 15 °, respectively. As can be seen in Fig. 3a, the microstructure of the alloy after two-passes of ECAP is composed of a small number of grains having HAGBs and a significantly large number of cells with LAGBs. As the occurrence of dynamic recrystallization (DRX) during ECAP to a cumulative strain of two at room temperature was unlikely, the HAGBs could be considered as the retained boundaries of the initial grains that became elongated during the two-pass ECAP process. The average size of the cells was calculated to be 900 nm.

By increasing the number of ECAP passes to six, more extensive grain refinement and cell formation occurred. In fact, the initial grains in the α-Al matrix became hardly discernible. The formation of a homogeneous nanostructure was indicated by extensive cell formation

and the presence of fine, nanosized and equiaxed grains. The average cell size was measured to be 82 nm. In addition, 68% of the grain boundaries are HAGBs.

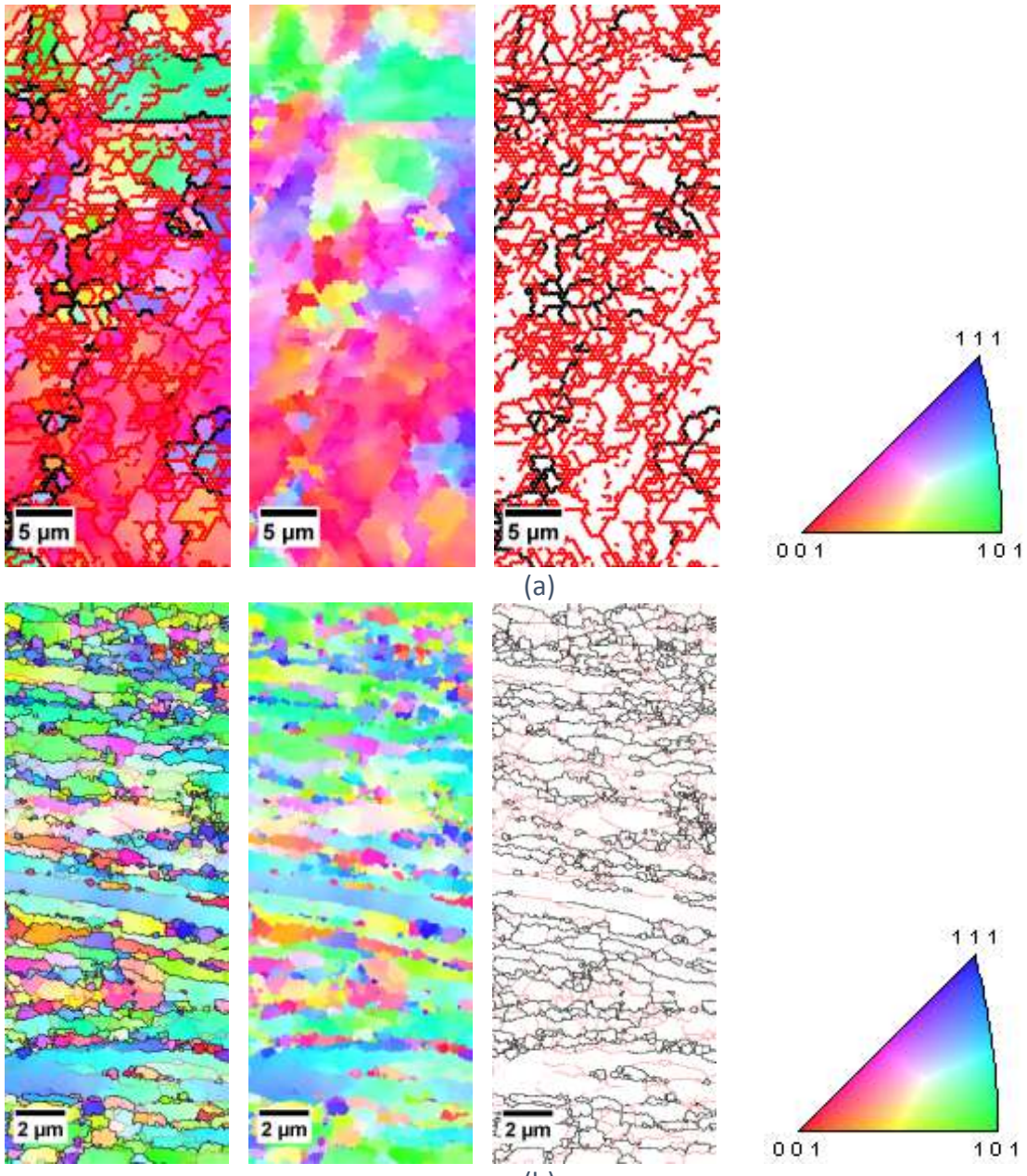

Figure 3 EBSD maps showing the nanostructures of the AA6063 alloy after (a) two and (b) six passes of ECAP. Micrographs were taken on the longitudinal section of the samples.

3.3 Hardness changes with increasing number of ECAP passes

The hardness values of the samples after two, four and six passes of ECAP, shown in Fig. 4, were all higher than the hardness value of the alloy after the two-pass ECAP and thermal

treatment (45 HBN). By applying two passes of ECAP, the hardness of the alloy increased to 68 HBN, which was a 51 % increase, contributed by work hardening. With increasing number of ECAP passes to four, the hardness value was elevated to 95.6 HBN. A further increase of the ECAP pass number to six led to a further increase of hardness to 99.5 HBN. In short, the hardness of the material showed an upward trend up to six passes of ECAP. This finding was however inconsistent with the results obtained from a previous study on this alloy [17] which showed that, after a small number of ECAP passes, the hardness of the alloy became unchanged [17]. It was reported that, for the AA6063 alloy, after an equivalent strain of 3 to 4, structural saturation occurred [14, 19]. It should be noted that, for aluminum, the equivalent strain where saturation occurs is significantly lower than that for other metals, e.g., copper, i.e., 15 [19]. In the case of pure aluminum, a maximum in strength was reached at an equivalent strain of two [20,21], followed by a reduction and then a plateau at an equivalent strain of six.

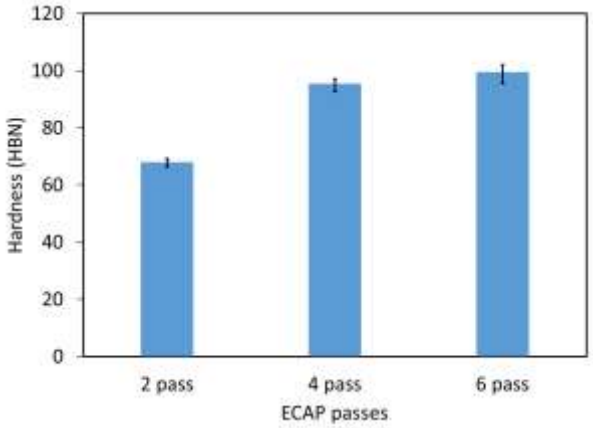

Figure 4 Variation of hardness with the number of ECAP passes.

The structural saturation has been attributed to a sequence of metallurgical phenomena occurring during an SPD process [19,22]. As deformation begins, subgrains form through dislocation multiplication and accumulation within the grains. As deformation continues, subgrain sizes decrease due to rapid increases in dislocation density. In the meantime, the

misorientation angles of subgrains increase and their boundaries become well distinguishable. At this stage, no further change in hardness will occur although further strain is imposed; the material enters a steady-state situation without further hardness evolution. This steady-state situation is attributed to the balance between the hardness increase due to the accumulation of dislocations and the decrease due to recrystallization, leading to fewer dislocations within individual grains, e.g., in the case of pure copper during SPD [19]. In the most extreme case, e.g., pure aluminum after two passes of ECAP, a maximum in the hardness curve was observed, followed by the reductions with increasing number of ECAP passes [20,21].

The formation of subgrains during an SPD process is in turn determined by dislocation mobility and affected by the following three factors [19]: (i) the presence of impurity elements, (ii) the difference in stacking fault energy (SFE) and (iii) the difference in the homologous temperature. The delayed occurrence of structural saturation observed in the present research might be related to the fine initial grain structure with a large area of grain boundaries that were capable of accommodating a large number of excess dislocations generated by dislocation multiplication during continuing SPD.

3.4 Changes of tensile properties with increasing number of ECAP passes

The engineering and true stress-strain curves of the material after the initial two-pass ECAP and thermal treatment are shown in Fig. 5a. The values of 0.2% offset yield strength (YS) and ultimate tensile strength (UTS) are 159.4 and 167.8 MPa, respectively. The material was quite ductile and its uniform elongation (e_u) and elongation to failure (e_f) were 3.48 and

10.79 %, respectively. The strain-hardening exponent, *n*, extracted from the true strain-stress curve, is shown in Fig. 5b. The calculated values of *n* and *K* are in agreement with the values found in the literature [23].

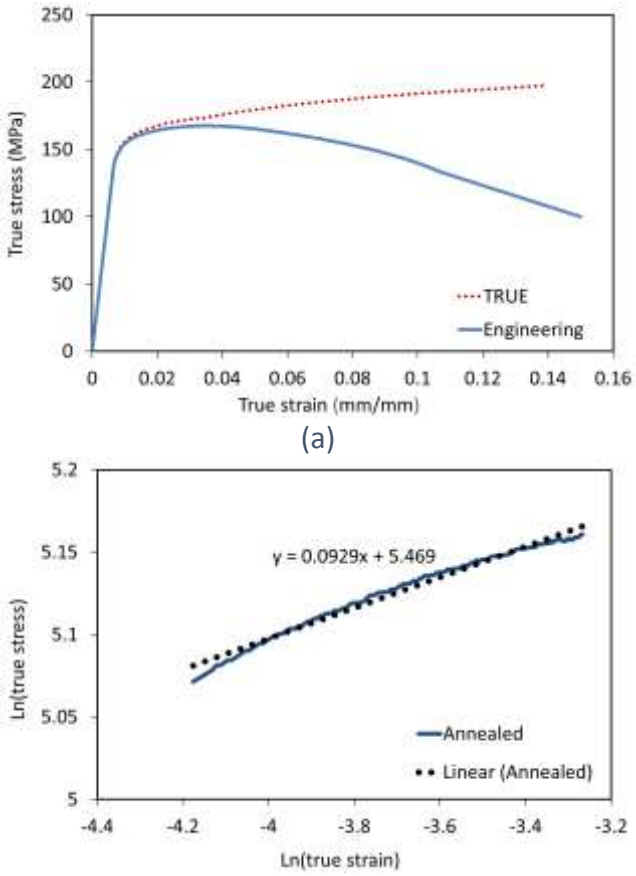

Figure 5 (a) Stress-strain curves of the AA6063 aluminum alloy after the initial two-pass ECAP and thermal treatment and (b) extraction of the *n* and *K* values.

The engineering stress-strain curves of the material after further ECAP through different passes are shown in Fig. 6. The values of YS, UTS, e_u and e_f are compared in Fig. 7. It is clear that both YS and UTS increased with increasing number of ECAP passes. YS increased from 197 MPa in the as-solution-treated state to 217 MPa after two passes of ECAP and to 310 MPa after six passes of ECAP. The increases in YS could be attributed to work hardening caused by cold deformation during ECAP, as has been observed in various metals and alloys [10,24–26]. The gradual increases in YS and UTS up to six passes of ECAP without showing

any sign of structural saturation were in line with the observation of the hardness change. Normally, with increasing number of ECAP passes, more deformation is imposed on the material and increases in hardness, YS and UTS are expected to occur due to strain hardening. In the present case, the trends of YS and UTS with increasing number of ECAP passes (Fig. 7a) were interesting. In fact, the difference between YS and UTS after two ECAP passes was very small, i.e., 1.7 %, which corresponded to a small value of uniform elongation e_u (Fig. 7b). It indicated that plastic instability occurred immediately after the material started plastic deformation. The difference became larger, as the number of ECAP passes increased to four and to six, i.e., 13.5 and 15.7 %, respectively.

The peculiar mechanical behavior of an SPD processed material has been reported [10,24–26]. In fact, high flow stress and low work hardening rate are related to a low ability of a UFG material to accumulate dislocations in the grain interior [8,9]. When a material undergoes a large amount of plastic deformation, e.g., an effective strain of two (i.e., two consecutive ECAP passes in the present research), it has already been deformed to an extent more than the amount of deformation that it can endure before localized deformation and necking occur. At this strain, the material with a low strain hardening exponent exhibits localized deformation due to its low ability to accumulate dislocations in the grain interior [8,9]. In the present research, a similar behavior was observed of the material in YS and UTS after four and six passes of ECAP. A noticeable difference concerned the increases in e_u along with increasing number of ECAP passes (Fig. 7b). This is in disagreement with the findings reported in the open literature that tensile elongation reduces with increasing stain during ECAP and other SPD processes [10,24–26]. As e_u is governed by the strain-hardening exponent [16], e_u may be improved, if the strain-

hardening exponent *n* increases with increasing number of ECAP passes. Therefore, the initial fine grain structure created by the two-pass ECAP and thermal treatment could be used to account for the improvements in elongation with increasing number of ECAP passes, because a large number of grain boundaries acted as obstacles to dislocations and promoted strain hardening. Although further grain refinement occurred during further ECAP passes, as shown in Fig. 3, the impact of the fine initial grain structure remained active. In addition, extensive grain refinement occurred during further passes of ECAP, as shown in Fig. 3, causing extensive dislocation annihilation and evacuation of the structure from dislocations during the deformation process. The resultant grain structure contained a lower density of dislocations, which facilitated the continuation of deformation, resulting in larger values of UTS, e_u and e_f with increasing number of ECAP passes.

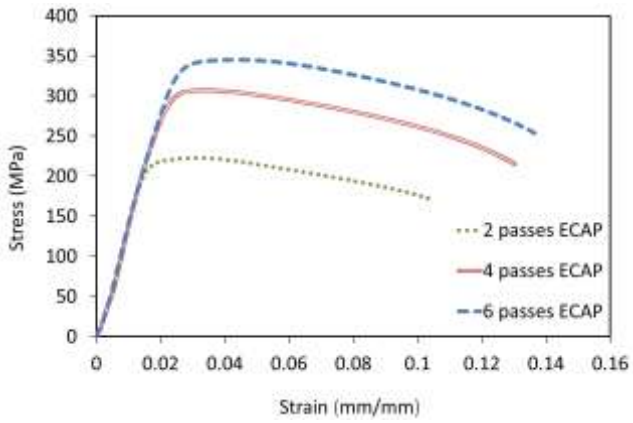

Figure 6 Engineering stress-strain curves of the material after two, four and six passes of ECAP.

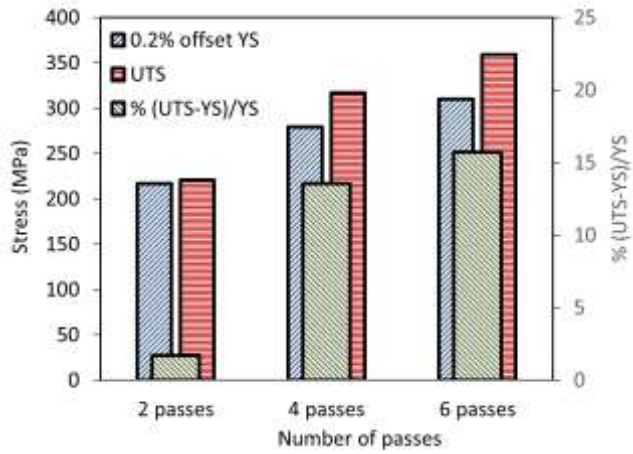

(a)

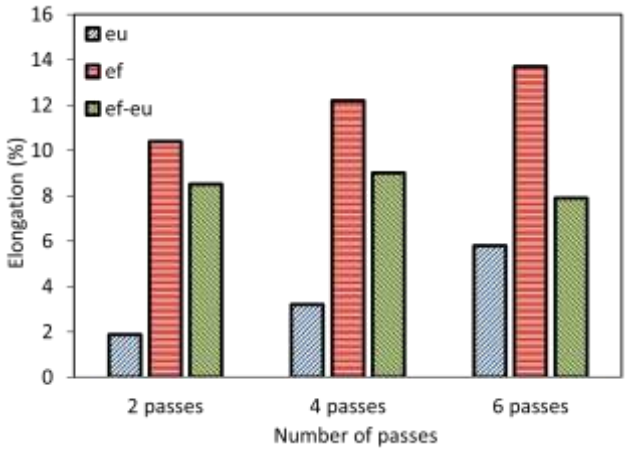

(b)

Figure 7 Effect of the number of ECAP passes on (a) YS and UTS and (b) e_u and e_f as well as their differences (e_f-e_u).

It has been reported that tensile elongation may be improved by increasing work-hardening rate [27,28], or creating a bimodal distribution of grain sizes [10-13, 30], or introducing nanoprecipitates [30] or enhancing solute enrichment [31,32]. Being different from the approaches taken in the previous research, the present research shows that a fine initial grain structure can indeed be utilized to enhance the ductility of the AA6063 alloy during subsequent SPD. It can be observed in Fig. 7b that e_f is much larger than e_u. The e_f value after two passes of ECAP is 10.4 % and it increases to 13.7 % after six passes of ECAP. This indicates that the material can resist a considerable amount of localized deformation in the necked region before failure. It should be noted that the uniform elongation is determined by the competition between plastic flow and material's resistance to localized plastic flow, while the elongation to failure is governed by the competition between localized plastic flow and fracture processes [33]. It can be seen in Fig. 7b that the e_f-e_u values that reflect the deformation in the localized deformation region are all very large, indicating that the specimens could resist fracture to great extents. Since the e_f-e_u values are nearly the same for the specimens after two, four and six passes of ECAP, it can be concluded that e_u, in

addition to its inherent significance for avoiding catastrophic failure, determines the e_f-e_u difference. Therefore, the following discussion on tensile elongation is focused on e_u.

In order to gain a better understanding of the reasons for the immediate occurrence of necking, small e_u values and, more importantly, the increases in elongation with increasing number of ECAP passes, the true stress-strain curves of the alloy, shown in Fig. 8, were used for the extraction of the *n* values, because *n* is a parameter useful for understanding the early occurrence of necking as well as the postponed failure. Comparison between Fig. 5a and Fig. 8 showed that, similar to the engineering stress-strain curves, the initial solution-treated material had the lowest flow stress but the largest e_f value. The true stress of the material increased with increasing number of ECAP passes and no saturation of tensile strengths occurred. The reason for the strength changes was basically the same as that for the hardness changes, as explained earlier. It has been reported that, in the case of the AA6063 alloy, the equivalent strain imposed during ECAP processing before saturation occurs is 3-4 [14, 19]. Fig. 8, however, shows that the material continues to strain harden even up to six passes of ECAP. This may be explained when the mechanism of strengthening introduced by SPD is considered. It is well known [16] that an increase in dislocation density at the starting passes of ECAP occurs, due to a large amount of strain imposed, leading to the formation of dislocation tangles. Consequently, further deformation governed by the movement of free dislocations becomes harder. This effect would be observed from the increases in hardness and YS and the decrease in elongation that occurred after two passes of ECAP, when Fig. 6 was compared with Fig. 5a. With further ECAP deformation, dislocation density increases to a point where the structure cannot endure further increases in dislocation density and cell formation starts. The substructure at this stage mainly consists

of the cells surrounded by boundaries with low misorientation angles. This explanation was confirmed by the EBSD results shown in Fig. 3. Further increases in strain may result in the formation of new grains with HAGBs. Obviously, this is unlike to occur at once. Rather, the fraction of HAGBs increases gradually. At this stage, the transformation of the cellular structure (Fig. 3) to a UFG structure occurs. In fact, when the dislocation density in the cell walls reaches a critical value, partial annihilation of dislocations of different signs occurs at the cell boundaries. Considering this mechanism of strengthening, one may understand that with a reduction in grain size through the two-pass ECAP and thermal treatment, the whole process of grain refinement occurring during subsequent ECAP would be accelerated, thus being beneficial for the increases in strength with increasing number of ECAP passes. In addition, the microstructures of aluminum and its alloys with an average grain size of 100 μm may become saturated after 3 to 4 passes of ECAP [14, 19], while other metals and alloys with fine initial grain structures, i.e., Mg, Fe and Cu, attend the saturated microstructures after a larger number of passes. Therefore, the fine initial structure of the AA6063 alloy created by applying the two-pass ECAP and thermal treatment delayed the occurrence of structural saturation and thus allowed its strength to increase up to six passes of ECAP.

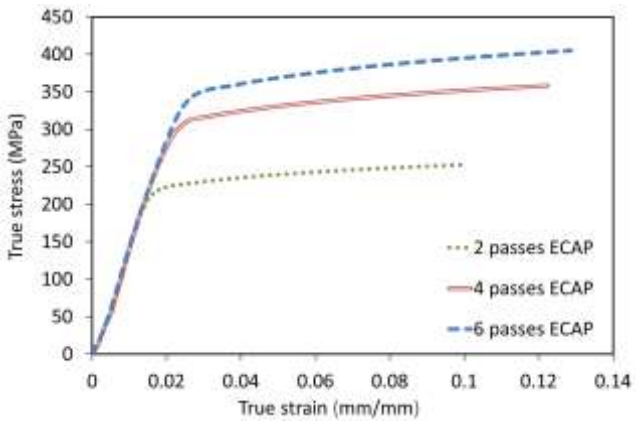

Figure 8 True stress-true strains curves of the ECAP-processed AA6063 aluminum alloy after different ECAP passes.

The strain hardening exponent *n*, extracted from the tensile curves, is plotted against the number of ECAP passes in Fig. 9. The calculated values of *n* and *K* are in line with those in the literature [23]. The *n* value is normally expected to reduce with increasing cold working to large strains. In the present research, however, the *n* value is seen to increase with increasing number of ECAP passes. In fact, after the sixth pass of ECAP, the *n* value (0.9991) even exceeded the initial value after the thermal treatment (0.0929) (Fig. 5b).

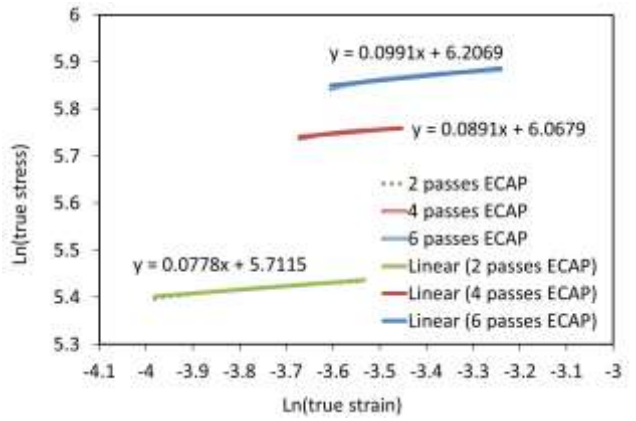

(a)

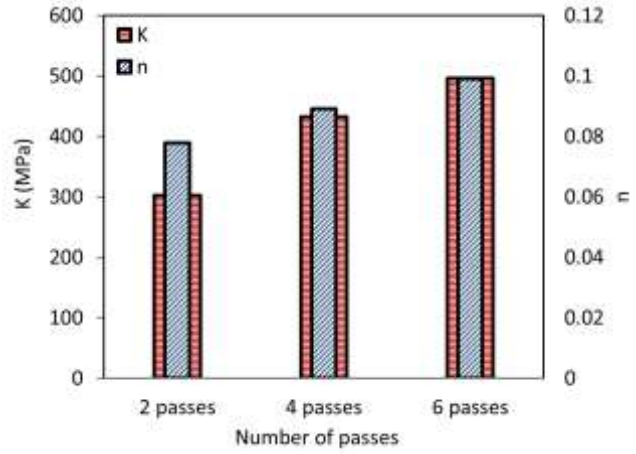

(b)

Figure 9 (a) Extraction of n and k after ECAP and (b) comparison between the *n* and *K* values.

4 Conclusions

In this research, the refinement of the initial grain structure of the AA6063 aluminum alloy with a high degree of supersaturation was proposed to serve as an alternative approach to achieving simultaneous improvements in its strength and ductility. In this connection, thermomechanical processing composed of two-pass ECAP and a thermal treatment was performed to generate a fine recrystallized grain structure with the alloying elements supersaturated in the α-Al solid solution. Thereafter, the billets were subjected to further ECAP processing. The effect of the number of ECAP passes on the hardness and tensile properties of the material was investigated. The results obtained have led to the following conclusions.

1- Structure saturation and unchanged hardness and tensile strengths, which normally occur to the alloy after 3-4 passes of ECAP, were not observed. This was attributed to the accommodation of a large number of excess dislocations generated through dislocation multiplication during ECAP by a larger area of grain boundaries in the fine initial grain structure. As a result, the strengths of the alloy kept increasing with increasing number of ECAP passes.
2- The ductility of the alloy was found to increase with increasing number of ECAP passes. This was attributed to the formation of a nanosized cellular structure with a large area of high-angle grain boundaries developed from the fine initial grain structure formed during the two-pass ECAP and thermal treatment applied earlier.

Acknowledgments

The authors would like to thank Prof. Nobuhiro Tsuji, Kyoto University, Japan, for providing equipment for EBSD analysis. The authors are also thankful from Japan Student Services

Organization (JASSO) for their support by Follow-up Research Fellowship in fiscal year of 2015.

References

[1] Z. Horita, T. Fujinami, M. Nemoto, T.G. Langdon, Improvement of mechanical properties for Al alloys using equal-channel angular pressing, J. Mater. Process. Technol. 117 (2001) 288–292.

[2] Z. Horita, T. Fujinami, M. Nemoto, T.G. Langdon, Equal-channel angular pressing of commercial aluminum alloys: grain refinement, thermal stability and tensile properties, Metall. Mater. Trans. A. 31 (2000) 691–701.

[3] S. Qu, X.H. An, H.J. Yang, C.X. Huang, G. Yang, Q.S. Zang, Z.G. Wang, S.D. Wu, Z.F. Zhang, Microstructural evolution and mechanical properties of Cu–Al alloys subjected to equal channel angular pressing, Acta Mater. 57 (2009) 1586–1601.

[4] N. Lugo, N. Llorca, J.M. Cabrera, Z. Horita, Microstructures and mechanical properties of pure copper deformed severely by equal-channel angular pressing and high pressure torsion, Mater. Sci. Eng. A. 477 (2008) 366–371.

[5] F. Dalla Torre, R. Lapovok, J. Sandlin, P.F. Thomson, C.H.J. Davies, E.V. Pereloma, Microstructures and properties of copper processed by equal channel angular extrusion for 1–16 passes, Acta Mater. 52 (2004) 4819–4832.

[6] L. Jin, D. Lin, D. Mao, X. Zeng, W. Ding, Mechanical properties and microstructure of AZ31 Mg alloy processed by two-step equal channel angular extrusion, Mater. Lett. 59 (2005) 2267–2270.

[7] W.J. Kim, C.W. An, Y.S. Kim, S.I. Hong, Mechanical properties and microstructures of an AZ61 Mg Alloy produced by equal channel angular pressing, Scr. Mater. 47 (2002) 39–44.

[8] E. Ma, Eight routes to improve the tensile ductility of bulk nanostructured metals and alloys, Jom. 58 (2006) 49–53.

[9] Y. Zhao, Y. Zhu, E.J. Lavernia, Strategies for improving tensile ductility of bulk nanostructured materials, Adv. Eng. Mater. 12 (2010) 769–778.

[10] S.K. Panigrahi, R. Jayaganthan, Development of ultrafine grained Al–Mg–Si alloy with enhanced strength and ductility, J. Alloys Compd. 470 (2009) 285–288.

[11] M. Zha, Y. Li, R.H. Mathiesen, R. Bjørge, H.J. Roven, High ductility bulk nanostructured Al–Mg binary alloy processed by equal channel angular pressing and inter-pass annealing, Scr. Mater. (2015). http://www.sciencedirect.com/science/article/pii/S1359646215001608 (accessed June 26, 2015).

[12] M. Zha, Y. Li, R.H. Mathiesen, R. Bjørge, H.J. Roven, Achieve high ductility and strength in an Al–Mg alloy by severe plastic deformation combined with inter-pass annealing, Mater. Sci. Eng. A. 598 (2014) 141–146.

[13] Y. Wang, M. Chen, F. Zhou, E. Ma, High tensile ductility in a nanostructured metal, Nature. 419 (2002) 912–915.

[14] S.M. Ashrafizadeh, A.R. Eivani, Correlative evolution of microstructure, particle dissolution, hardness and strength of ultrafine grained AA6063 alloy during annealing, Mater. Sci. Eng. A. 644 (2015) 284–296.

[15] A.R. Eivani, S. Ahmadi, E. Emadoddin, S. Valipour, A.K. Taheri, The effect of deformations passes on the extrusion pressure in axi-symmetric equal channel angular extrusion, Comput. Mater. Sci. 44 (2009) 1116–1125.
[16] G.E. Dieter, Mechanical metallurgical, McGraw-Hill Boston MA. (1986) 290.
[17] S.M. Ashrafizadeh, A.R. Eivani, Correlative evolution of microstructure, particle dissolution, hardness and strength of ultrafine grained AA6063 alloy during annealing, Mater. Sci. Eng. A. In press. (2015). doi:10.1016/j.msea.2015.06.074.
[18] M. Das, G. Das, M. Ghosh, M. Wegner, V. Rajnikant, S. GhoshChowdhury, T.K. Pal, Microstructures and mechanical properties of HPT processed 6063 Al alloy, Mater. Sci. Eng. A. 558 (2012) 525–532.
[19] K. Edalati, T. Fujioka, Z. Horita, Microstructure and mechanical properties of pure Cu processed by high-pressure torsion, Mater. Sci. Eng. A. 497 (2008) 168–173.
[20] Y. Harai, Y. Ito, Z. Horita, High-pressure torsion using ring specimens, Scr. Mater. 58 (2008) 469–472.
[21] Y. Ito, Z. Horita, Microstructural evolution in pure aluminum processed by high-pressure torsion, Mater. Sci. Eng. A. 503 (2009) 32–36.
[22] R.Z. Valiev, R.K. Islamgaliev, I.V. Alexandrov, Bulk nanostructured materials from severe plastic deformation, Prog. Mater. Sci. 45 (2000) 103–189.
[23] A. Sivaraman, U. Chakkingal, Flow properties of an aluminum alloy processed by equal channel angular pressing, J. Mater. Sci. 43 (2008) 7432–7437.
[24] E.A. El-Danaf, M.S. Soliman, A.A. Almajid, M.M. El-Rayes, Enhancement of mechanical properties and grain size refinement of commercial purity aluminum 1050 processed by ECAP, Mater. Sci. Eng. A. 458 (2007) 226–234.
[25] D.R. Fang, Z.F. Zhang, S.D. Wu, C.X. Huang, H. Zhang, N.Q. Zhao, J.J. Li, Effect of equal channel angular pressing on tensile properties and fracture modes of casting Al–Cu alloys, Mater. Sci. Eng. A. 426 (2006) 305–313.
[26] T.L. Tsai, P.L. Sun, P.W. Kao, C.P. Chang, Microstructure and tensile properties of a commercial 5052 aluminum alloy processed by equal channel angular extrusion, Mater. Sci. Eng. A. 342 (2003) 144–151.
[27] Y.M. Wang, E. Ma, Three strategies to achieve uniform tensile deformation in a nanostructured metal, Acta Mater. 52 (2004) 1699–1709.
[28] I. Sabirov, M.R. Barnett, Y. Estrin, P.D. Hodgson, The effect of strain rate on the deformation mechanisms and the strain rate sensitivity of an ultra-fine-grained Al alloy, Scr. Mater. 61 (2009) 181–184.
[29] G.J. Fan, H. Choo, P.K. Liaw, E.J. Lavernia, Plastic deformation and fracture of ultrafine-grained Al–Mg alloys with a bimodal grain size distribution, Acta Mater. 54 (2006) 1759–1766.
[30] Y.-H. Zhao, X.-Z. Liao, S. Cheng, E. Ma, Y.T. Zhu, Simultaneously increasing the ductility and strength of nanostructured alloys, Adv. Mater.-DEERFIELD BEACH THEN Weinh.-. 18 (2006) 2280.
[31] R.Z. Valiev, M.Y. Murashkin, A. Kilmametov, B. Straumal, N.Q. Chinh, T.G. Langdon, Unusual super-ductility at room temperature in an ultrafine-grained aluminum alloy, J. Mater. Sci. 45 (2010) 4718–4724.
[32] C.M. Hu, C.M. Lai, P.W. Kao, N.J. Ho, J.C. Huang, Solute-enhanced tensile ductility of ultrafine-grained Al–Zn alloy fabricated by friction stir processing, Scr. Mater. 60 (2009) 639–642.

[33] I. Sabirov, M.Y. Murashkin, R.Z. Valiev, Nanostructured aluminium alloys produced by severe plastic deformation: New horizons in development, Mater. Sci. Eng. A. 560 (2013) 1–24.